frontiers | Frontiers in Physics

TYPE Brief Research Report
PUBLISHED 16 September 2024
DOI 10.3389/fphy.2024.1446803

OPEN ACCESS

EDITED BY
Karol Krzempek,
Wrocław University of Science and Technology, Poland

REVIEWED BY
Livio Gianfrani,
Università degli Studi della Campania Luigi Vanvitelli, Italy
Antonio Castrillo,
University of Campania Luigi Vanvitelli, Italy

*CORRESPONDENCE
Davide Gatti,
davide1.gatti@polimi.it

RECEIVED 10 June 2024
ACCEPTED 26 August 2024
PUBLISHED 16 September 2024

CITATION
Gotti R, Wójtewicz S, Marangoni M, Gatti D and Lamperti M (2024) High-precision HD spectroscopy near 1.53 μm.
Front. Phys. 12:1446803.
doi: 10.3389/fphy.2024.1446803

High-precision HD spectroscopy near 1.53 μm

Riccardo Gotti[1], Szymon Wójtewicz[2], Marco Marangoni[3], Davide Gatti[3]* and Marco Lamperti[4]

[1]Dipartimento di Ingegneria Industriale e dell'Informazione, Università di Pavia, Pavia, Italy, [2]Institute of Physics, Faculty of Physics, Astronomy and Informatics, Nicolaus Copernicus University, Toruń, Poland, [3]Dipartimento di Fisica - Politecnico di Milano and IFN-CNR, Lecco, Italy, [4]Dipartimento di Scienza e Alta tecnologia, Università degli studi dell'Insubria, Como, Italy

In this study, we report highly precise and accurate measurements of the P(5), P(6), and O(3) transitions of the 2–0 band of HD occurring at approximately 1.5 μm. HD spectra were acquired in the pressure range of 100–900 Torr using a cavity ring-down spectrometer linked to an optical frequency comb. The line-shape analysis was performed using the Hartmann–Tran profile in the so-called β-corrected version. For the P(5) transition, we improved the accuracy of previous line center frequency determinations by more than two orders of magnitude. Moreover, for the P(5) and P(6) line centers, the total standard uncertainty is below 3 MHz, similar to those provided by quantum electrodynamics predictions, making them useful for direct comparisons that might foster future improvements of the theoretical model.

KEYWORDS

precision molecular spectroscopy, HD spectroscopy, cavity ring-down spectroscopy, optical frequency comb, line position

1 Introduction

In the past 2 decades, molecular spectroscopy has experienced a paradigmatic change with the invention of the optical frequency comb. On one hand, these combs enabled the accurate determination of atomic and molecular transition energies at unprecedented levels [1, 2] over a large portion of the electromagnetic spectrum, from the near-IR to the mid-IR [3, 4]. On the other hand, they ensure the linearity and repeatability of the frequency axis in spectroscopic measurements, providing a reliable basis for the comparison of the results. Due to optical frequency combs, a variety of fundamental physics applications have become possible, including high-accuracy Doppler broadening thermometry (DBT) [5–12] and tests of quantum electrodynamics (QED) on molecules [13–15].

Among the most scientifically interesting spectroscopic targets, molecular hydrogen is a benchmark for direct comparisons of QED calculations with experimental investigations [14–16] due to its simple molecular structure. A major hurdle when dealing with molecular hydrogen is related to the symmetry of its electronic ground state, making electric dipole transitions forbidden for homo-nuclear species (H_2, D_2, and T_2) or very weak for hetero-nuclear isotopologs (HD, DT, and HT). In addition, modeling absorption lines is non-trivial for measurements in both Doppler-broadening and sub-Doppler regimes. In the first case, this is due to the requirement to include collisional effects [17] or even hyperfine structure effects [18] in the model and the need to extrapolate the line centers to zero pressure [19–21]. In the second case, to achieve accuracy at the few kHz level, the model has to include line asymmetries that were subject to different interpretations, either in terms of the underlying hyperfine structure and crossover resonances [14] or Fano resonances [15].

Although the adoption of optical frequency combs provides the desired accuracy for the horizontal (frequency) axis, optical cavities with very high finesse can be used to achieve the desired sensitivity for the vertical (absorption) axis. Optical cavities strongly enhance the interaction path between light and molecules, extending it up to the kilometer level [22, 23], thus improving the signal-to-noise ratio (SNR) of weak transition measurements. Among cavity-enhanced approaches like cavity mode-width spectroscopy (CMWS) [24], cavity mode-dispersion spectroscopy (CMDS) [25], and NICE-OHMS [26], cavity ring-down spectroscopy (CRDS) is the technique adopted in this work. CRDS is based on the comparative measurement of the cavity photon lifetime with and without absorption from the sample, with the advantage of being highly resilient against frequency and amplitude laser noise while also giving access to the absolute absorption coefficient without the need for any cavity-length calibration [27]. With this technique, sensitivity levels below $6 \cdot 10^{-11}$ cm^{-1} have been achieved with relatively simple implementations [28, 29] and down to $5 \cdot 10^{-13}$ cm^{-1} in the best conditions [30].

In this paper, we investigate three lines of the HD isotopologue with relatively high rotational quantum numbers, namely, the P(5), P(6), and O(3) lines of the 2–0 band with theoretical transition frequencies of 6,576.900679 cm^{-1}, 6,458.91050 cm^{-1}, and 6,636.161018 cm^{-1}, respectively, as reported by H2SPECTRE software [31]. These values correspond to a natural abundance of 0.0311432% (according to HITRAN). We provide the most accurate, up-to-date experimental determination of their transition frequencies. For the P(5) line, in particular, our measurement shows an accuracy improved by two orders of magnitude with respect to the available literature data [32]. For both P(5) and P(6), the final uncertainty is at the MHz level, and this sets conditions for a meaningful comparison with theory. Due to the very weak line intensities, namely, $2.548 \cdot 10^{-31}$ cm/molecule for P(5), $2.054 \cdot 10^{-32}$ cm/molecule for P(6), and $2.78 \cdot 10^{-32}$ cm/molecule for O(3), measurements have been conducted in a Doppler broadening regime. The absorption spectra were measured over a wide pressure range, from 100 to 900 Torr, using a CRD spectrometer linked to an optical frequency comb. The line-shape analysis was performed using the computationally cost-effective Hartmann–Tran profile [17, 33], modified for the so-called β correction [34, 35]. To reduce the numerical correlations between the large number of fitted collisional parameters, we performed a series of multispectrum fits [36]. The uncertainty budget takes into account the uncertainty of the line shape model and collisional parameters, whether fixed or left free (for which *ab initio* values are not available).

2 Experimental setup and data analysis procedure

The HD absorption profiles were acquired using a comb-assisted CRD spectrometer, as reported in [19, 29]. In brief, the setup includes a 50 cm-long high finesse (>120,000) cavity, thermally stabilized at 300.65 K, which houses the gas under investigation, namely, hydrogen enriched in deuterium (D 97%) with a purity of 98%, and all the measurements are performed under static conditions. Its length can be slowly controlled using a piezoelectric (PZT) actuator. The probe laser is an extended-cavity diode laser (TOPTICA DL pro, tunable from 1.5 to 1.63 μm) that can be frequency-agile tuned using a single-sideband-modulator (SSM) driven by an RF synthesizer (AnaPico APSIN 12G) over a radio-frequency range of approximately 12 GHz, with a total output power of almost 20 mW after passing through an optical amplifier (Thorlabs BOA1004S). The probe beam is dither-locked to a cavity resonance through frequency modulation of the single sideband with a depth of ±4 MHz. Once a given threshold is reached at the photo-detector (Thorlabs PDB450C, gain 10^6 V/W with 300 kHz bandwidth) outside the cavity, a ring-down event is started by simultaneously switching off both the SSM and an acousto-optic modulator (AOM). A first set of ring-down events is measured using the so-called frequency-agile-rapid-scanning approach [37]: when a predefined number of decay constants is acquired, the SSM is shifted by a cavity free spectral range (FSR) (approximately 300 MHz) to continue the acquisition on the next resonance. Once a sufficient span needed to acquire the entire absorption line and its tails is completed, the probe beam frequency is slowly shifted by 50 MHz, while the dither lock servo adjusts the cavity length. Then, another series of FSR-spaced decay constants is acquired, and this interleaving procedure is repeated until a final spectrum of interleaved points separated by 50 MHz is obtained.

Absorption spectra were measured for each line at five pressures: 100, 300, 500, 700, and 900 Torr, at a temperature of 300.65 K. The signal-to-noise ratio achieved in the measurements depends on both the measurement pressure and the absorption coefficient of the specific line and ranges from 920 to 8,500 for the P(5) line, from 100 to 850 for the P(6) line, and from 140 to 860 for the O(3) line.

The analysis of the spectra was based on the Hartmann–Tran profile [17, 33], which goes beyond the commonly used Voigt profile, adding the speed dependence of pressure broadening and shifting in the quadratic approximation, the velocity-changing collisions leading to Dicke narrowing, and correlations between velocity- and phase-changing collisions. Specifically, we used the so-called β-corrected Hartmann–Tran profile (βHTP) to fit all three lines since it was shown to accurately reproduce the spectra of hydrogen isotopologues. This profile is an approximation of the more physically justified and accurate speed-dependent billiard-ball profile [38] and improves the hard-collision hypothesis considered in the standard HTP without adding any extra parameter or increasing the computational cost [34, 35, 39]. Due to the high number of line-shape parameters describing the model, large correlations among them typically arise when fitting a single spectrum. For example, the line profile asymmetry caused by the collisional effects can be modeled by adopting more than one parameter, albeit nonphysical values for some of them can be obtained. To mitigate this effect and obtain a robust result for the zero-pressure transition frequency, we performed a global fit of the spectra acquired at multiple pressures (multispectrum fit) as this considerably reduces the correlations between fitted values [36]. In particular, we enforced the expected linear dependence of the collisional parameters on pressure. For the lines investigated, no collisional parameter was available from quantum-scattering *ab initio* calculations to further constrain the fitting procedure. Therefore, we performed the fitting in a variety of conditions, progressively reducing the number and the subset of free

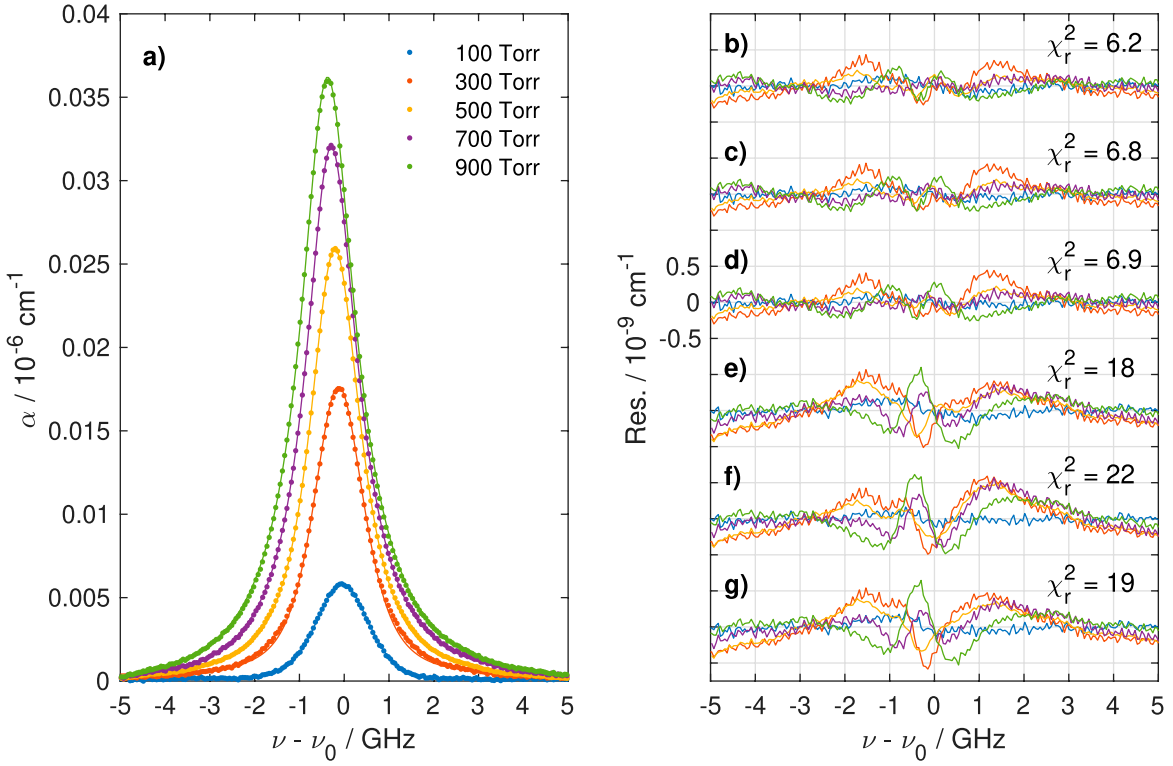

FIGURE 1
Multispectrum fit of the O(3) line. **(A)** Data (with baseline and interfering line subtracted for clarity) fitted with β-HTP without any constraint on the collisional parameters. **(B)** Residuals of the fit (data-fit) without constraints. The reduced χ^2 value is indicated in the label. **(C)** Residuals of the fit when fixing $\eta = 0$. **(D)** Residuals of the fit when fixing $\eta, \Im\{\nu_{VC}\} = 0$. **(E)** Residuals of the fit when $\delta_2, \gamma_2, \eta = 0$. **(F)** Residuals of the fit when $\delta_2, \gamma_2, \eta, \Im\{\nu_{VC}\} = 0$. **(G)** Residuals of the fit when $\Re\{\nu_{VC}\}$ is fixed to the value calculated from the diffusion coefficient [41] and $\eta = 0$.

collisional parameters, to find the best balance between the fit quality, the consistency of the parameters obtained from the fit, and the physical coherence of the constraints on the fixed parameters. First, we decided to neglect the correlations between velocity- and phase-changing collisions by setting the η parameter to 0. Second, we fixed the imaginary part of the Dicke narrowing parameter to 0 since, for molecular hydrogen, this is often small compared to other parameters [40]. Additionally, we evaluated whether the speed dependence of collisional broadening and shifting (represented by γ_2 and δ_2, respectively) could be neglected to check whether the recorded spectra could be modeled with only the Dicke effect. Finally, we evaluated the impact of setting the real part of the Dicke narrowing parameter (ν_{VC}) to the value calculated from the diffusion coefficient of HD [41].

We identified the best type of fit by monitoring the value of the resulting χ^2 and the fit quality factor (QF) [42], calculated for each pressure value as the ratio between the signal amplitude and the standard deviation of the fit residuals. In the case of a fit with flat residuals, the QF equals the SNR of the measurement. We identified the choice of constraints that minimizes χ^2, while minimizing the number of fitting parameters, as the best-fit condition. In our case, the use of other goodness-of-fit estimators, such as the Bayesian or Akaike information criterion, results in the same outcome for model selection. This is due to the relatively large number of spectral points (about 200 per pressure), implying that the number of degrees of freedom is about the same when fixing some of the fit parameters. The reported zero-pressure center frequency is the frequency retrieved by such a fit.

The overall fit model includes the HD line expressed with a β-HTP profile along with a cubic baseline. When necessary, we included additional interfering lines from H_2O and C_2H_2, modeled using the Voigt profile and/or a saw-tooth baseline [29]. In all the figures, the contribution of these features has been subtracted from the data for clarity. In particular, we added two extra lines for the data analysis of the P(5) and P(6) transitions and one extra line plus a saw-tooth baseline for the O(3) transition.

3 Results

For each line, we evaluated the quality of different fit constraints by monitoring the values of χ^2 and QF. The results for the O(3) line are shown in Figure 1. We found that there was no noticeable reduction in the fit quality when fixing $\eta = 0$ or $\eta, \Im\{\nu_{VC}\} = 0$ compared to the fit with all free parameters, as shown in Figures 1B–D. We also noticed that the fitted collisional parameters do not vary significantly in these three cases, suggesting that these parameters do not play a significant role in modeling our data and can be safely fixed to 0. We attribute the systematic structure

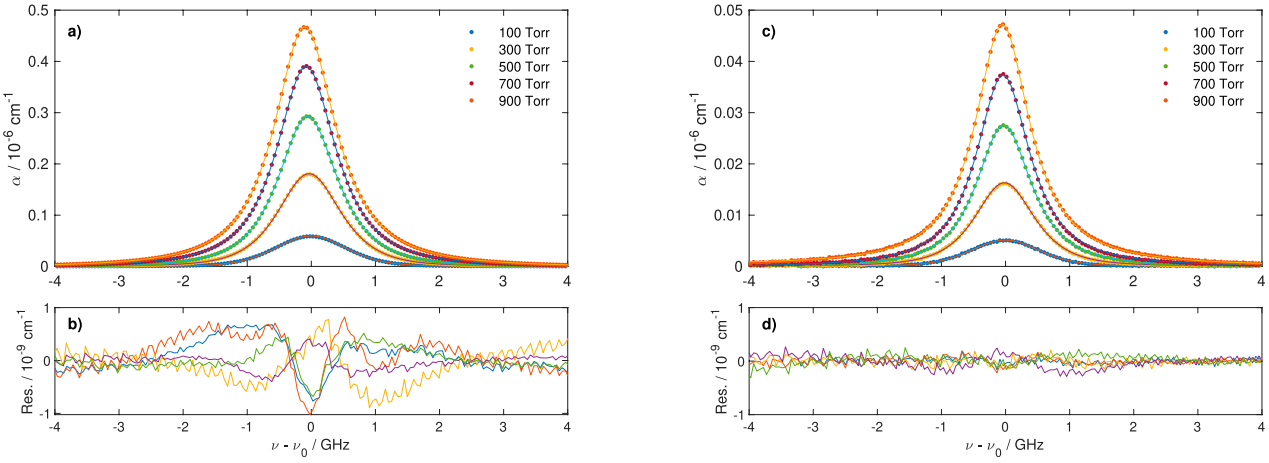

FIGURE 2
Multispectrum fits of the P(5) and P(6) lines, with η and $\Im\{\nu_{VC}\}$ fixed to 0. **(A)** Experimental data and fits for the P(5) line and **(B)** fit residuals. **(C)** Experimental data and fits for the P(6) line and **(D)** fit residuals. Note the variation in the vertical axis of a factor of 10 between panels **(A)** and **(C)** and the corresponding noisier residuals in **(D)**. The increased noise level partially hides systematic deviations in the residuals for the P(6) line (panel **(D)**).

TABLE 1 Collisional parameters obtained from the multipressure fits of the three lines analyzed.

Parameter	P(5)	P(6)	O(3)
γ_0	0.0089(3)	0.011(1)	0.021(2)
δ_0	−0.00241(3)	−0.00092(8)	−0.0083(2)
γ_2	0.0033(9)	0.008(2)	0.012(2)
δ_2	0.00073(7)	0.00050(9)	0.0010(3)
$\Re\{\nu_{VC}\}$	0.025(4)	0.019(2)	0.005(5)

The values of $\Im\{\nu_{VC}\}$ and η are fixed to 0. Units are cm^{-1}/bar for all parameters. Presented uncertainties take into account the statistical contribution obtained from the fit routine and the systematic contributions from the modeling of the baseline and interfering lines.

found in the residuals at a level of about 1% of the line amplitude to the intrinsic limitations of β-HTP used for modeling line shapes of H_2 isotopologues [19, 20]. When fixing the speed dependence of pressure broadening and shift to 0 or when fixing $\Re\{\nu_{VC}\}$ to the value determined from the diffusion coefficient [41], the fit quality decreased significantly (see panels Figures 1E–G). This confirms that for molecular hydrogen, the collisional effects, especially the speed dependence of collisional shift and velocity-changing collisions, are very pronounced. As a consequence, all the collisional parameters, except for η and $\Im\{\nu_{VC}\}$, cannot be fixed to 0 and need to be fitted to the data due to the lack of a reliable source for their values. This analysis led us to choose the third fit configuration (i.e., with $\eta, \Im\{\nu_{VC}\} = 0$) for the determination of the line center frequency at zero pressure as it provides nearly the highest QF with the fewest fitting parameters.

The results of similar fits for the P(5) and P(6) lines are shown in Figure 2. The systematic structure in the residuals is more evident for the P(5) transition, primarily due to its higher line strength. Conversely, the P(6) line shows smaller residuals than the O(3) line even if it is characterized by a comparable line strength. In Table 1, we report the fitted collisional parameters for all three lines. The reported uncertainty on the collisional parameters takes into account the statistical uncertainty and the uncertainty from modeling the baseline and interfering lines. The procedure for evaluating these contributions is the same as the one described in detail for the transition frequency in the next paragraph.

To determine the uncertainty on the retrieved transition frequencies, we considered various contributing factors of errors. The statistical contribution component (type A) has been estimated from the covariance matrix returned by the fitting routine. We identified five main sources of systematic uncertainty (type B): the line-shape model, the choice of the constrained collisional parameters in the fit, the uncertainty on the thermodynamic parameters of the gas inside the cavity, the influence of the baseline and that of interfering lines. Other sources, like the stability of the reference Rb clock or the noise of the optical frequency comb used for frequency referencing, are negligible. To evaluate the effect of the specific line-shape model chosen for fitting, β-HTP, we repeated all fits using a standard HTP model. We retained the difference between the transition frequencies retrieved with the two models as an estimate of the maximum error due to the choice of the model. Regarding the effect of fixing both η and $\Im\{\nu_{VC}\}$ to 0, we took the maximum discrepancy between the values of ν_0 obtained from the first three fit configurations (i.e., without fixing any collisional parameters, fixing $\eta = 0$, or fixing both $\eta = 0$ and $\Im\{\nu_{VC}\} = 0$) as an estimate of the error related to the choice of the constrained fit parameters. The error due to the uncertainty in pressure reading σ_p translates into an error on the retrieved transition frequency by multiplying it with the linear pressure shift δ_0 retrieved from the fit. Regarding the uncertainty in temperature reading, it has no direct effect on the fitted transition frequency. Instead, it artificially modifies the retrieved collisional parameters, which are a function of temperature. The most significant effect is an error in the

TABLE 2 Uncertainty budget including both statistical (Type A) and systematic (Type B) contributions for the positions of the HD 2–0 band P(5), P(6), and O(3) transitions.

	P(5)	P(6)	O(3)
Type A	0.31	0.82	1.44
Type B	0.81	0.36	8.68
Model	0.75	0.24	0.09
Collisional	0.27	0.26	8.66
Pressure	0.14	0.06	0.50
Baseline	0.64	1.17	2.68
Interfering lines	0.09	1.65	1.6
Total	1.08	2.21	9.33

All values are 1σ uncertainties given in MHz.

retrieved δ_0, which, in turn, affects the estimation of the error stemming from the pressure uncertainty. The error in the measured temperature, σ_T, can be propagated to the error on δ_0 using

$$\frac{\partial \delta_0}{\partial T} = \frac{3}{T}\delta_2,$$

from Equation (4) in [34]. This contribution to the total uncertainty is about 1/100 or less than that of the pressure reading and can be neglected. To evaluate the uncertainty associated with the baseline model, we repeated the fits, replacing the cubic baseline with a linear baseline plus an etalon. This model gave slightly worse results than the cubic baseline. We considered the difference between the transition frequencies evaluated in these ways as the error due to baseline modeling. Finally, to evaluate the error due to interfering lines, we repeated the fit, fixing the center of the interfering lines to the value found from HITRAN.

Our final accuracy is approximately 1 MHz for the P(5) transition, 2 MHz for the P(6) transition, and 9 MHz for the O(3) transition. Even better results (especially for the O(3) transition) could be achieved by performing *ab initio* quantum scattering calculations of the line-shape parameters and utilizing them in the data analysis. This would mitigate systematics given by the complex collisional physics of molecular hydrogen in the high-pressure range. However, this is outside the scope of this paper. Another solution could be performing measurements in the low-pressure range in which the atypical shapes of molecular hydrogen transitions are less pronounced. Such a solution would require the development of a more sensitive spectrometer.

Table 2 reports the uncertainty budget and combined uncertainty for the lines measured in this study, while Table 3 reports the retrieved line center frequency compared to the theoretical QED value provided by H2SPECTRE [31]. For the P(5) line, which, to the best of our knowledge, was the only one previously measured, we provide an improved determination [32]. The comparison with that unique experimental determination of the P(5) transition shows a discrepancy of approximately 1σ of combined uncertainty (note that it translates to a high absolute value of this discrepancy), dominated by the uncertainty described in [32]. To the best of our knowledge, the P(6) and O(3) lines have been measured for the first time in this study. The discrepancies between measured and theoretical transition frequencies range between a minimum of 1.6 MHz for the P(6) line and a maximum of 6.3 MHz for the P(5) line. For the P(6) line, the discrepancy is comparable with that measured in other transitions [20, 43, 44] and suggests an underestimation of the line center in the theoretical models. For the O(3) line, the discrepancy is below 1σ due to the large experimental uncertainty. Finally, the discrepancy found for the P(5) line is less clear: although its sign is coherent with recent measurements of other lines in the literature, its magnitude is significantly larger. The comparison with the literature is not helpful since the uncertainty of the only previous determination is more than two orders of magnitude larger. Further investigations are needed to clarify the source of this uncertainty, such as the calculation of *ab initio* collisional parameters and comparison with the fit results obtained in this study and/or measurements at lower pressures.

4 Conclusion

We have presented the first highly precise and accurate comb-assisted measurement of the P(5), P(6), and O(3) transitions in the 2-0 band of the HD molecule at 1.53 μm. The measurements were performed using a CRDS spectrometer in a wide pressure range spanning from 100 to 900 Torr. The recorded data were analyzed using the β-corrected Hartmann–Tran profile. We retrieved transition frequencies with uncertainties of 1.1, 2.2, and 9.3 MHz for the P(5), P(6), and O(3) lines, respectively. In the case of the P(5) transition, our result represents more than a 200-fold improvement compared to previously available data. All the transition frequencies determined in this work are a few MHz higher than those obtained from theoretical calculations. This discrepancy is consistent with the results from various

TABLE 3 Comparison of experimental and theoretical determinations of the HD 2–0 band P(5), P(6), and O(3) transition frequencies. All given values are in MHz.

	P(5)	P(6)	O(3)
Experimental—this work	197170528.4(1.1)	193633373.5(2.2)	198947107.9(9.3)
Theoretical—H2SPECTRE [31]	197170522.1(9)	193633371.9(9)	198947102.3(9)
Experimental—[32]	197170382(240)		
Δ_{E-T}	6.3	1.6	5.6
Δ_{E-E}	146.4		

studies on different bands and suggests limitations in the theoretical models.

Data availability statement

The raw data supporting the conclusions of this article will be made available by the authors, without undue reservation.

Author contributions

RG: conceptualization, data curation, investigation, methodology, resources, software, validation, writing–original draft, writing–review and editing, and supervision. SW: investigation, methodology, validation, writing–review and editing, formal analysis, software, and writing–original draft. MM: conceptualization, funding acquisition, project administration, writing–review and editing, supervision, and writing–original draft. DG: investigation, software, writing–original draft, writing–review and editing, and methodology. ML: conceptualization, data curation, formal analysis, project administration, software, supervision, validation, visualization, writing–original draft, and writing–review and editing.

Funding

The author(s) declare that financial support was received for the research, authorship, and/or publication of this article. The authors acknowledge financial support by the European Union's NextGenerationEU Programme with the I-PHOQS Infrastructure (IR0000016, ID D2B8D520, CUP B53C22001750006) Integrated infrastructure initiative in PHOtonic and Quantum Sciences.

Conflict of interest

The authors declare that the research was conducted in the absence of any commercial or financial relationships that could be construed as a potential conflict of interest.

Publisher's note

All claims expressed in this article are solely those of the authors and do not necessarily represent those of their affiliated organizations, or those of the publisher, the editors, and the reviewers. Any product that may be evaluated in this article, or claim that may be made by its manufacturer, is not guaranteed or endorsed by the publisher.

References

1. Holzwarth R, Udem T, Hänsch TW, Knight J, Wadsworth W, Russell PSJ. Optical frequency synthesizer for precision spectroscopy. *Phys Rev Lett* (2000) 85:2264–7. doi:10.1103/physrevlett.85.2264

2. Diddams SA, Jones DJ, Ye J, Cundiff ST, Hall JL, Ranka JK, et al. Direct link between microwave and optical frequencies with a 300 THz femtosecond laser comb. *Phys Rev Lett* (2000) 84:5102–5. doi:10.1103/physrevlett.84.5102

3. Fortier T, Baumann E. 20 years of developments in optical frequency comb technology and applications. *Commun Phys* (2019) 2:153. doi:10.1038/s42005-019-0249-y

4. Lamperti M, Gotti R, Gatti D, Shakfa MK, Cané E, Tamassia F, et al. Optical frequency metrology in the bending modes region. *Commun Phys* (2020) 3:175. doi:10.1038/s42005-020-00441-y

5. Gotti R, Lamperti M, Gatti D, Marangoni M. Laser-based primary thermometry: a review. *J Phys Chem Reference Data* (2021) 50. doi:10.1063/5.0055297

6. Gotti R, Lamperti M, Gatti D, Wójtewicz S, Puppe T, Mayzlin Y, et al. Multispectrum rotational states distribution thermometry: Application to the 3ν1+ν3 band of carbon dioxide. *New J. Phys.* (2020). 22:083071. doi:10.1088/1367-2630/aba85d

7. Gotti R, Moretti L, Gatti D, Castrillo A, Galzerano G, Laporta P, et al. Cavity-ring-down Doppler-broadening primary thermometry. *Phys Rev A* (2018) 97:012512. doi:10.1103/physreva.97.012512

8. Gianfrani L. Linking the thermodynamic temperature to an optical frequency: recent advances in Doppler broadening thermometry. *Philos Trans R Soc A: Math Phys Eng Sci* (2016) 374:20150047. doi:10.1098/rsta.2015.0047

9. De Vizia MD, Odintsova T, Gianfrani L. Hyperfine structure effects in Doppler-broadening thermometry on water vapor at 1.4 μm. *Metrologia* (2016) 53:800–4. doi:10.1088/0026-1394/53/2/800

10. Hashemi R, Povey C, Derksen M, Naseri H, Garber J, Predoi-Cross A. Doppler broadening thermometry of acetylene and accurate measurement of the Boltzmann constant. *J Chem Phys* (2014) 141:214201. doi:10.1063/1.4902076

11. Castrillo A, Fasci E, Dinesan H, Gravina S, Moretti L, Gianfrani L. Optical determination of thermodynamic temperatures from a C_2H_2 line-doublet in the near infrared. *Phys Rev Appl* (2019) 11:064060. doi:10.1103/physrevapplied.11.064060

12. Gatti D, Mills AA, De Vizia MD, Mohr C, Hartl I, Marangoni M, et al. Frequency-comb-calibrated Doppler broadening thermometry. *Phys Rev A - At Mol Opt Phys* (2013) 88:012514. doi:10.1103/physreva.88.012514

13. Cozijn F, Dupré P, Salumbides E, Eikema K, Ubachs W. Sub-Doppler frequency metrology in HD for tests of fundamental physics. *Phys Rev Lett* (2018) 120:153002. doi:10.1103/physrevlett.120.153002

14. Diouf M, Cozijn F, Darquié B, Salumbides E, Ubachs W. Lamb-dips and Lamb-peaks in the saturation spectrum of HD. *Opt Lett* (2019) 44:4733–6. doi:10.1364/ol.44.004733

15. Hua TP, Sun Y, Hu SM. Dispersion-like lineshape observed in cavity-enhanced saturation spectroscopy of HD at 1.4 μm. *Opt Lett* (2020) 45:4863–6. doi:10.1364/ol.401879

16. Salumbides E, Dickenson G, Ivanov T, Ubachs W. QED effects in molecules: test on rotational quantum states of H_2. *Phys Rev Lett* (2011) 107:043005. doi:10.1103/physrevlett.107.043005

17. Ngo N, Lisak D, Tran H, Hartmann JM. An isolated line-shape model to go beyond the Voigt profile in spectroscopic databases and radiative transfer codes. *J Quantitative Spectrosc Radiative Transfer* (2013) 129:89–100. doi:10.1016/j.jqsrt.2013.05.034

18. Castrillo A, Fasci E, Gianfrani L. Doppler-limited precision spectroscopy of HD at 1.4 μm: an improved determination of the R(1) center frequency. *Phys Rev A* (2021) 103:022828. doi:10.1103/physreva.103.022828

19. Wójtewicz S, Gotti R, Gatti D, Lamperti M, Laporta P, Jóźwiak H, et al. Accurate deuterium spectroscopy and comparison with *ab initio* calculations. *Phys Rev A* (2020) 101:052504. doi:10.1103/physreva.101.052504

20. Lamperti M, Rutkowski L, Ronchetti D, Gatti D, Gotti R, Cerullo G, et al. Stimulated Raman scattering metrology of molecular hydrogen. *Commun Phys* (2023) 6:67. doi:10.1038/s42005-023-01187-z

21. Lamperti M, Rutkowski L, Gatti D, Gotti R, Moretti L, Polli D, et al. A stimulated Raman loss spectrometer for metrological studies of quadrupole lines of hydrogen isotopologues. *Mol Phys* (2023) 121:e2196353. doi:10.1080/00268976.2023.2196353

22. Romanini D, Ventrillard I, Méjean G, Morville J, Kerstel E. Introduction to cavity enhanced absorption spectroscopy. In: *Cavity-enhanced spectroscopy and sensing*. Springer (2014). p. 1–60.

23. Gianfrani L, Hu SM, Ubachs W. Advances in cavity-enhanced methods for high precision molecular spectroscopy and test of fundamental physics. *La Rivista Del Nuovo Cimento* (2024) 47:229–98. doi:10.1007/s40766-024-00054-z

24. Cygan A, Lisak D, Morzyński P, Bober M, Zawada M, Pazderski E, et al. Cavity mode-width spectroscopy with widely tunable ultra narrow laser. *Opt Express* (2013) 21:29744–54. doi:10.1364/oe.21.029744

25. Cygan A, Wcisło P, Wójtewicz S, Masłowski P, Hodges JT, Ciuryło R, et al. One-dimensional frequency-based spectroscopy. *Opt Express* (2015) 23:14472–86. doi:10.1364/oe.23.014472

26. Ye J, Ma LS, Hall JL. Ultrasensitive detections in atomic and molecular physics: demonstration in molecular overtone spectroscopy. *J Opt Soc America B: Opt Phys* (1998) 15:6–15. doi:10.1364/josab.15.000006

27. O'Keefe A, Deacon DA. Cavity ring-down optical spectrometer for absorption measurements using pulsed laser sources. *Rev Scientific Instr* (1988) 59:2544–51. doi:10.1063/1.1139895

28. Gatti D, Sala T, Gotti R, Cocola L, Poletto L, Prevedelli M, et al. Comb-locked cavity ring-down spectrometer. *J Chem Phys* (2015) 142:074201. doi:10.1063/1.4907939

29. Gotti R, Gatti D, Masłowski P, Lamperti M, Belmonte M, Laporta P, et al. Conjugating precision and acquisition time in a Doppler broadening regime by interleaved frequency-agile rapid-scanning cavity ring-down spectroscopy. *J Chem Phys* (2017) 147:134201. doi:10.1063/1.4999056

30. Kassi S, Campargue A. Cavity ring down spectroscopy with 5×10^{-13} cm^{-1} sensitivity. *J Chem Phys* (2012) 137:234201. doi:10.1063/1.4769974

31. Komasa J, Puchalski M, Czachorowski P, Łach G, Pachucki K. Rovibrational energy levels of the hydrogen molecule through nonadiabatic perturbation theory. *Phys Rev A* (2019) 100:032519. doi:10.1103/physreva.100.032519

32. Lin T, Chou CC, Lwo DJ, Shy JT. Absorption spectrum of the P(5) transition of the first overtone band of HD. *Phys Rev A* (2000) 61:064502. doi:10.1103/physreva.61.064502

33. Tennyson J, Bernath PF, Campargue A, Császár AG, Daumont L, Gamache RR, et al. Recommended isolated-line profile for representing high-resolution spectroscopic transitions (IUPAC Technical Report). *Pure Appl Chem* (2014) 86:1931–43. doi:10.1515/pac-2014-0208

34. Wcisło P, Gordon I, Tran H, Tan Y, Hu SM, Campargue A, et al. The implementation of non-Voigt line profiles in the HITRAN database: H_2 case study. *J Quantitative Spectrosc Radiative Transfer* (2016) 177:75–91. doi:10.1016/j.jqsrt.2016.01.024

35. Konefał M, Słowiński M, Zaborowski M, Ciuryło R, Lisak D, Wcisło P. Analytical-function correction to the Hartmann–Tran profile for more reliable representation of the Dicke-narrowed molecular spectra. *J Quantitative Spectrosc Radiative Transfer* (2020) 242:106784. doi:10.1016/j.jqsrt.2019.106784

36. Benner DC, Rinsland CP, Devi VM, Smith MAH, Atkins D. A multispectrum nonlinear least squares fitting technique. *J Quantitative Spectrosc Radiative Transfer* (1995) 53:705–21. doi:10.1016/0022-4073(95)00015-d

37. Truong GW, Douglass KO, Maxwell SE, van Zee RD, Plusquellic DF, Hodges JT, et al. Frequency-agile, rapid scanning spectroscopy. *Nat Photon* (2013) 7:532–4. doi:10.1038/nphoton.2013.98

38. Ciuryło R, Shapiro DA, Drummond JR, May AD. Solving the line-shape problem with speed-dependent broadening and shifting and with Dicke narrowing. II. Application. *Phys Rev A* (2001) 65:012502. doi:10.1103/physreva.65.012502

39. Wcisło P, Thibault F, Stolarczyk N, Jóźwiak H, Słowiński M, Gancewski M, et al. The first comprehensive dataset of beyond-Voigt line-shape parameters from *ab initio* quantum scattering calculations for the HITRAN database: He-perturbed H_2 case study. *J Quantitative Spectrosc Radiative Transfer* (2021) 260:107477. doi:10.1016/j.jqsrt.2020.107477

40. Wcisło P, Thibault F, Zaborowski M, Wójtewicz S, Cygan A, Kowzan G, et al. Accurate deuterium spectroscopy for fundamental studies. *J Quantitative Spectrosc Radiative Transfer* (2018) 213:41–51. doi:10.1016/j.jqsrt.2018.04.011

41. Amdur I, Beatty JJ. Diffusion coefficients of hydrogen isotopes. *J Chem Phys* (1965) 42:3361–4. doi:10.1063/1.1695735

42. Cygan A, Lisak D, Wójtewicz S, Domysławska J, Hodges JT, Trawiński RS, et al. High-signal-to-noise-ratio laser technique for accurate measurements of spectral line parameters. *Phys Rev A* (2012) 85:022508. doi:10.1103/physreva.85.022508

43. Mondelain D, de Casson LB, Fleurbaey H, Kassi S, Campargue A. Accurate absolute frequency measurement of the S(2) transition in the fundamental band of H_2 near 2.03 μm. *Phys Chem Chem Phys* (2023) 25:22662–8. doi:10.1039/d3cp03187j

44. Fleurbaey H, Koroleva A, Kassi S, Campargue A. The high-accuracy spectroscopy of H_2 rovibrational transitions in the (2–0) band near 1.2 μm. *Phys Chem Chem Phys* (2023) 25:14749–56. doi:10.1039/d3cp01136d